Proton and Metal Ion Interactions with Glycylglycylhistamine, a Serum Albumin Mimicking Pseudopeptide

Tamás Gajda,*,† Bernard Henry,*,‡ André Aubry,§ and Jean-Jacques Delpuech‡

Department of Inorganic and Analytical Chemistry, Attila József University, H-6701 Szeged, P. O. Box 440, Hungary, LESOC, URA CNRS 406, Université Henri Poincaré Nancy I, B.P. 239, F-54506 Vandoeuvre-lès-Nancy Cedex, France, and Laboratoire de Minéralogie, Cristallographie et Physique Infrarouge, URA CNRS 809, Université Henri Poincaré Nancy I, B.P. 239, F-54506 Vandoeuvre-lès-Nancy Cedex, France

Received March 31, 1995[⊗]

The macro- and microprotonations of glycylglycylhistamine (GGHA) have been determined by combined potentiometric and ^{1}H-NMR methods. The complexation of GGHA with Co(II), Ni(II), and Cu(II) has been studied by potentiometric, EPR, and ^{1}H-NMR methods. In the pH range 3−11.2, more or less deprotonated monomeric complexes (MLH, ML, MLH_{-1}, MLH_{-2}, MLH_{-3}) formed in all systems. In the case of Ni(II) and Cu(II) at physiological pH, the MLH_{-2} species is predominant with four nitrogen coordination sites (one amino, two peptide, and one imidazole-N^3 nitrogens) in square planar arrangement. In Co(II) containing systems however, CoL is the predominant complex near pH 7 with a macrochelate coordination of terminal amino and imidazole nitrogens, while $CoLH_{-2}$ species forms at much higher pH. In accordance with NMR measurements, the formation of MLH_{-3} species can be assigned to the further deprotonation of the N^1-pyrrolic nitrogen in the imidazole ring without metal coordination. The formation constants determined were compared with those of the analogous histidine derivatives. Single-crystal X-ray analysis of $CuLH_{-2}\cdot 3H_2O$ verified the expected four nitrogen coordination in the equatorial plane of Cu(II).

Introduction

Serum albumin (SA) has been considered to operate the transport of trace metals between tissues and blood.[1] The copper(II) transport site of human serum albumin (HSA) involves the α-NH_2 nitrogen, the two peptide nitrogens, and the imidazole nitrogen of the N-terminal Asp-Ala-His residue.[2−4] Additionnal coordination by the carboxyl side chain of the aspartyl residue seems to be still controversial (see refs 5 and 6). Copper(II) complexes of simple tripeptides mimicking this binding site, Gly-Gly-His,[7−12] Gly-Gly-His-*N*-methylamide[13,14] (gghma), and the native sequence Asp-Ala-His-*N*-methylamide[15] (aahma), have been extensively studied in both a thermodynamic and structural[14] point of view. The $CuLH_{-2}$ species (coordinated by the above mentioned four nitrogens) is an important complex in all the systems reported; however, the results are contradictory concerning the other species formed, even for the same equilibrium system. Generally, the formation of bis-complexes and some minor species is disputed. For example, in the Cu(II)−Gly-Gly-His system, Farkas *et al.*[11] reported the single $CuLH_{-2}$ species at pH ≥ 3, while Lau and Sarkar[9] suggest the formation of 10 complexes. The equilibrium study of Cu(II)−Gly-Gly-His (and Ni(II)−Gly-Gly-His) complexes is further complicated by an oxidative decarboxylation of the ligand.[16] The X-ray structure investigation of the Cu(II)−gghma complex[14] showed a distorted square-planar structure involving four nitrogens from one ligand molecule—in the same manner as has been proposed for the Cu(II)-binding site of serum albumin—with a weak axial water coordination.

Although Ni(II) and Co(II) are known to be able to compete with Cu(II) for this specific binding site of HSA,[6,17] little attention was paid to the Ni(II)[12,18] or Co(II)[19] complexes of serum albumin mimicking peptides.

In previous publications[20−23] on the coordination properties of histamine-containing pseudodipeptides, we obtained results completing our knowledge on the acid−base properties, on the structure of complexes formed with this type of peptides and on the role of the carboxylate group in coordination. This paper describes solution equilibrium and spectroscopic (UV−vis, EPR, and NMR) behaviors of proton, Co(II), Ni(II) and Cu(II) complexes of glycylglycylhistamine (GGHA). Possible struc-

* Authors to whom correspondence should be addressed.
† Attila József University.
‡ URA CNRS 406.
§ URA CNRS 809.
⊗ Abstract published in *Advance ACS Abstracts,* December 15, 1995.

(1) Bearn, A. G.; Kunkel, H. G. *Proc. Soc. Exp. Biol.* **1954**, *85*, 44.
(2) Peters, T., Jr.; Blumenstock, F. A. *J. Biol. Chem.* **1967**, *242*, 1574.
(3) Neumann, P. Z.; Sass-Kortsak, A. *J. Clin. Invest*. **1967**, *46*, 646.
(4) Sarkar, B.; Wigfield, Y. *Can. J. Biochem.* **1968**, *46*, 601.
(5) Laussac, J. P.; Sarkar, B. *Biochemistry* **1984**, *23*, 2832.
(6) Sadler, P. J.; Tucker, A.; Viles, J. H. *Eur. J. Biochem.***1994**, *220*, 193.
(7) Aiba, H.; Yokoyama, A.; Tanaka, H. *Bull. Chem. Soc. Jpn.* **1974**, *47*, 1437.
(8) Kruck, T. P. A.; Sarkar, B. *Inorg. Chem.* **1975,** *14*, 2383.
(9) Lau, S.; Sarkar, B. *J. Chem. Soc., Dalton Trans.* **1981**, 491.
(10) Demaret, A.; Ensuque, A.; Lapluye, G. *J. Chim. Phys.* **1983**, *80*, 475.
(11) Farkas, E.; Sovago, I.; Kiss, T.; Gergely, A. *J. Chem. Soc., Dalton Trans.* **1984**, 611.
(12) Hay, R. W.; Hassan, M. M.; You-Quan, C. *J. Inorg. Biochem.* **1993**, *52*, 17.
(13) Kruck, T. P. A.; Lau, S.; Sarkar, B. *Can. J. Chem.* **1976**, *54*, 1300.
(14) Camerman, N.; Camerman, A.; Sarkar, B. *Can. J. Chem.* **1976**, *54*, 1309.
(15) Iyer, K. S.; Lau, S.; Laurie, S. H.; Sarkar, B. *Biochem. J.* **1978**, *169*, 61.
(16) de Meester, P.; Hodgson, D. G. *Inorg. Chem.* **1978**, *17*, 440.
(17) Kolthoff, I. F.; Willeford, B. R. *J. Am. Chem. Soc.* **1958**, *80*, 5673.
(18) Glennon, J. D.; Sarkar, B. *Biochem. J.* **1982**, *203*, 15.
(19) Lakusta, H.; Sarkar, B. *J. Inorg. Biochem.* **1979**, *11*, 303.
(20) Gajda, T.; Henry, B.; Delpuech, J. J. *J. Chem. Soc., Dalton Trans.* **1992**, 2313.
(21) Gajda, T.; Henry, B.; Delpuech, J. J. *J. Chem. Soc., Dalton Trans.* **1993**, 1301.
(22) Gajda, T.; Henry, B.; Delpuech, J. J. *J. Chem. Soc., Perkin Trans.2* **1994**, 157.
(23) Gajda, T.; Henry, B.; Delpuech, J. J. *Inorg. Chem.* **1995**, *34*, 2455.

0020-1669/96/1335-0586$12.00/0

tures of species formed in solution are also discussed together with X-ray structural studies of the $[CuGGHAH_{-2}]^*3H_2O$ complex.

Experimental Section

Materials. GGHA·2HCl was prepared from BOC-glycylglycine and histamine, according to the procedure described earlier.[24] The purity of GGHA·2HCl was checked by NMR measurements, elemental analysis, and acid−base titrations. ^{1}H-NMR data for GGHA·2HCl (in DMSO): N−H_{imid} (14.48 ppm), C8−H (9.05), N2−H (8.78), N3−H (8.28), N1−H_3 (∼8.25), C9−H (7.45), C6−H_2 (2.83), C5−H_2 (3.38), C3−H_2 (3.75) and C1−H_2 (3.61). No other signal was observed.

Stock solutions of metal perchlorates (Alpha Ventron products) were standardized complexometrically.

The red, crystalline $[CuGGHAH_{-2}]\cdot 3H_2O$ complex was crystallized from water containing copper(II) and GGHA in a 1:50 ratio, at pH = 8.0 standing at room temperature for about 1 week.

pH-Metric Measurements. The coordination equilibria were investigated by potentiometric titrations at 298.15 ± 0.1 K under nitrogen atmosphere at constant ionic strength (0.1 mol dm^{-3} $NaClO_4$). Changes in pH were followed by using an Orion (Catalog No. 91−03) combined glass electrode and an Orion 710 pH-meter (precision 0.1 mV). For the quantitative evaluation of the data, eq 1 was used between the experimental

$$E = E_0 + \frac{RT}{F}\ln[H^+] + j_H[H^+] + j_{OH}[H^+]^{-1}K_w \qquad (1)$$

electromotive force values (E) and the equilibrium hydrogen ion concentrations [H$^+$], where j_H and j_{OH} are fitting parameters in acidic and alkaline media for the correction of experimental errors, mainly due to the liquid-junction potential and to the possible alkaline and acidic errors of the glass electrode,[25] and K_w (= $10^{-13.75}$) is the autoprotolysis constant of water.[26]

The complex formation constants were calculated as the averages of 10 independent titrations. The metal ion to ligand ratios (R = [M]/[L]) were varied from 1:2 (from 1:1 in case of copper(II)) to 1:4, with metal ion concentrations between 2 × 10^{-3} and 1.2 × 10^{-2} mol dm^{-3}.

The species formed in the investigated systems can be characterized by the general equilibrium process (2) (charges

$$pM + qL + rH \leftrightarrow M_pL_qH_r \qquad (2)$$

omitted). The formation constants (β_{pqr}) for this generalized reaction were evaluated from the pH-metric titration data with the PSEQUAD computer program.[27]

Spectroscopic Measurement. The visible absorption spectra were recorded on a Varian DMS 100 UV−vis spectrophotometer. The EPR spectra were obtained on a Bruker ER-200 D spectrometer at room temperature and at 9.45 GHz. Proton, ^{13}C-, and ^{14}N-NMR spectra were recorded on a Bruker AM-400 spectrometer with dioxane (3.7 ppm for ^{1}H and 67.4 ppm for ^{13}C) and KNO_3 (0 ppm for ^{14}N) as internal standard. The study of microprotonation was performed in H_2O (I = 0.1 mol dm^{-3} $NaClO_4$), while D_2O was used in the case of metal complexes . The calculation of microconstants and other technical details of NMR measurements have been described earlier.[22]

Table 1. Details of Data Collection and Structure Refinement

compound	$CuGGHAH_{-2}\cdot 3H_2O$
formula	$CuC_9H_{13}N_5O_2\cdot 3H_2O$
molecular weight	340.83
crystal system	orthorhombic
a (Å)	18.808
b (Å)	14.227
c (Å)	10.142
vol of unit cell (Å$^{3)}$	2714
no. of molecules in unit cell	8
calcd density (g cm$^{-3)}$	1.67
space group	Pbcn
radiation	Cu Kα (λ = 1.541 78 Å)
tot. no. of reflcns	1993
no. of significant reflcns [$I > 3\sigma(I)$]	1406
refined params	183
R, R_w, GOF	0.032, 0.033, 1.59
max residual density (e Å^{-3})	0.6

Crystal Structure Determination. Intensities were collected, at room temperature, on a CAD4 diffractometer in the $\omega-2\theta$ scan mode ($\theta \leq 70°$). Lorentz and polarization corrections were applied. The structure was solved by the direct methods using the SHELX 76 software package.[28] Refined parameters were calculated by using anisotropic thermal parameters for non hydrogen atoms and isotropic factors for all hydrogen atoms. Cell dimensions together with other experimental conditions and residual factors are listed in Table 1. Positions of atoms and equivalent thermal parameters are given in Table 2. Main bond distances and angles are given in Table 3. All the crystallographic materials (atomic coordinates, bond lengths, bond angles, and equivalent thermal factors) have been deposited at the Cambridge Crystallographic Data Center.

Results and Discussion

Equilibrium Studies. Protonation. The pH-metrically determined macroscopic protonation constants K_1 and K_2 of the free ligand are listed in Table 4 as the formation constants β_{011} and β_{012}. They can be approximatively assigned to the protonation of the amino group and imidazole ring, respectively. As generally obtained for peptides, the pK of the terminal amino group is decreased compared to that of amino acids, due to the lack of hydrogen bonding with the carboxylate group. In this way, as the two protonation steps overlap significantly, an alternative microprotonation can also occur.[22] The microscopic protonation equilibria of amino (NH_2) and imidazole (ImH) groups are shown in Scheme 1. The corresponding protonation microconstants (represented also in Scheme 1) are related to macroconstants K_1 and K_2 as follows:[29]

$$K_1 = k^a + k^i \qquad (3)$$

$$K_1K_2 = k^ak^i_a = k^ik^a_i \qquad (4)$$

Additional information is required to evaluate all the constants in eq 3 and 4; this may be conveniently brought by ^{1}H-NMR spectroscopy: the chemical shifts of neighboring protons reflect the protonation states of both relevant proton-binding sites, independently because they are well separated by nine connecting atoms. In this work, the group-specific pH-profiles of the imidazole (H−C^2 and H−C^5) and the N-terminal methylenic

(24) Henry, B.; Gajda, T.; Selve, C.; Delpuech, J. J.; Arnould, J. M. *Amino Acids* **1993**, *5*, 113.
(25) Rosotti, F. J. C.; Rosotti, H. *The determination of stability constants;* McGraw-Hill Book Co.: New York, 1961; p 149.
(26) Högfeldt, E. *Stability Constants of Metal-ion Complexes, Part A, Inorganic Ligands;* Pergamon: New York, 1982; p 32.
(27) Zékány, L.; Nagypál, L. PSEQUAD. In *Computational Methods for the Determination of Stability Constants*; Legget, D., Ed.; Plenum: New York, 1985.
(28) Sheldrick, G. M. *SHELX 76. Program for Crystal Structure Determination*; University of Cambridge: Cambridge, England, 1976.
(29) Noszal, B. Acid−base properties of bioligands. In *Biocoordination Chemistry;* Burger, K., Ed.; Ellis Horwood: New York, London, 1990.

Table 2. Fractional Atomic Coordinates and Equivalent Thermal Parameters in the Cu(GGHAH$_{-2}$)·3H$_2$O Complex (Standard Deviations Given in Parentheses)

	x	*y*	*z*	B(Å^2)		*x*	*y*	*z*
Cu	0.21653(3)	0.12196(4)	0.12870(6)	2.15(1)	HN11	0.097(2)	0.197(3)	0.117(4)
N1	0.1089(2)	0.1289(2)	0.1443(3)	2.75(7)	HN12	0.079(2)	0.084(3)	0.086(4)
C1	0.087 (2)	0.1051(3)	0.2804(4)	2.66(9)	HN5	0.180(2)	0.108(2)	-0.358(4)
C2	0.1504(2)	0.0992(2)	0.3735(4)	2.19(8)	HO3	0.460(2)	0.193(2)	0.279(4)
O1	0.1390(1)	0.0820(2)	0.4938(3)	2.65(6)	HO41	0.068(2)	0.644(2)	0.491(4)
N2	0.2108(2)	0.1124(2)	0.3149(3)	2.11(7)	HO42	0.035(2)	0.625(3)	0.633(4)
C3	0.2778(2)	0.1098(3)	0.3858(4)	2.23(8)	HO5	0.539(2)	1.009(2)	0.218(4)
C4	0.3379(2)	0.1051(2)	0.2858(4)	2.21(9)	HO61	0.501(2)	0.343(3)	0.360(4)
O2	0.4009(1)	0.1009(2)	0.3303(3)	2.85(6)	HO62	0.547(2)	0.413(3)	0.460(4)
N3	0.3189(2)	0.1061(2)	0.1615(3)	2.23(7)	H11	0.064(2)	0.046(3)	0.279(3)
C5	0.3740(2)	0.1001(3)	0.0593(4)	2.52(9)	H12	0.056(2)	0.150(3)	0.310(4)
C6	0.3580(2)	0.1676(3)	-0.0526(4)	2.74(9)	H31	0.281(2)	0.055(3)	0.440(4)
C7	0.2909(2)	0.1473(3)	-0.1256(4)	2.41(8)	H32	0.286(2)	0.169(3)	0.439(4)
N4	0.2259(2)	0.1377(2)	-0.0613(3)	2.34(7)	H51	0.376(2)	0.034(2)	0.023(3)
C8	0.1779(2)	0.1235(3)	-0.1564(4)	2.71(9)	H52	0.421(2)	0.115(3)	0.103(4)
N5	0.2081(2)	0.1249(2)	-0.2747(3)	2.92(8)	H61	0.354(2)	0.224(3)	-0.023(4)
C9	0.2795(2)	0.1390(3)	-0.2558(4)	2.76(9)	H62	0.394(2)	0.167(3)	-0.111(4)
O3	0.500	0.2401(3)	0.250	3.9(1)	H81	0.129(2)	0.112(2)	-0.144(3)
O4	0.0655(2)	0.6733(2)	0.5841(3)	4.47(8)	H91	0.316(2)	0.140(3)	-0.322(4)
O5	0.500	0.9654(3)	0.250	3.5(1)				
O6	0.4979(2)	0.4042(2)	0.4150(3)	4.37(7)				

Table 3. Bond Lengths (Å) and Angles (deg) in the Cu(GGHAH$_{-2}$)·3H$_2$O Complex (Standard Deviations Given in Parentheses)

Cu−N1	2.034(3)	Cu−N2	1.897(3)
Cu−N3	1.968(3)	Cu−N4	1.948(3)
N1−C1	1.480(5)	C1−C2	1.523(5)
C2−O1	1.263(5)	C2−N2	1.295
N2−C3	1.452(5)	C3−C4	1.521(5)
C4−O2	1.268(4)	C4−N3	1.311(5)
N3−C5	1.467(5)	C5−C6	1.517(6)
C6−C7	1.492(5)	C7−N4	1.393(5)
C7−C9	1.343(6)	N4−C8	1.335(5)
C8−N5	1.328(5)	N5−C9	1.371(5)
N1−Cu−N2	82.5(1)	O2−C4−N3	126.6(3)
N1−Cu−N3	165.3(1)	Cu−N3−C4	115.5(3)
N1−Cu−N4	99.3(1)	Cu−N3−C5	125.3(3)
N2−Cu−N3	83.1(2)	C4−N3−C5	119.1(2)
N2−Cu−N4	176.9(1)	N3−C5−C6	110.6(3)
N3−Cu−N4	95.3(1)	C5−C6−C7	114.6(3)
Cu−N1−C1	109.7(3)	C6−C7−N4	122.0(3)
N1−C1−C2	111.9(2)	C6−C7−C9	129.8(3)
C1−C2−O1	118.5(4)	N4−C7−C9	108.2(4)
C1−C2−N2	113.2(4)	Cu−N4−C7	123.6(2)
O1−C2−N2	128.3(3)	Cu−N4−C8	129.5(3)
Cu−N2−C2	121.1(3)	C7−N4−C8	105.6(3)
Cu−N2−C3	116.4(2)	N4−C8−N5	111.2(3)
C2−N2−C3	122.1(3)	C8−N5−C9	107.1(3)
N2−C3−C4	108.5(3)	C7−C9−N5	107.8(3)
C3−C4−N3	116.0(3)		
Cu−N3−C4	115.5(3)		
N1−C1−C2−N2	−2.5(4)	C4−N3−C5−C6	−138.2(3)
C1−C2−N2−C3	179.9(3)	N3−C5−C6−C7	−63.3(4)
C2−N2−C3−C4	167.0(3)	C5−C6−C7−N4	53.5(5)
N2−C3−C4−N3	1.2(4)	C5−C6−C7−C9	−129.5(4)
C3−C4−N3−C5	−179.0(3)		

signals (Figure 1) were used to elucidate[22,29] the four protonation microconstants, which are as follows: log k^a = 7.77(02), log k^i = 7.04(02), log k_i^a = 7.62(02) and log k_a^i = 6.89(02). The pH-independent concentration ratio of the two monoprotonated micro-species HL (k^i/k^a) is 0.186, which corresponds to relative amounts of the minor protonation isomer ($ImH_2^+-NH_2$) of 15.7%. This result is particularly interesting concerning the metal binding site in MLH complexes (charges omitted), in line with the view that, besides the usually proposed imidazole coordination , the alternative amino-coordinated structure can also form (see later). The interactivity parameter (Δ = log k^a - log k_i^a = log k^i − log k_a^i) is characteristic for the influence of the protonation state of a given group on the basicity of the other protonation site. For histamine Δ was found[30] to be 1.02 reflecting the strong hydrogen-bond between amino and imidazole group in monoprotonated species. In a previous paper, we reported Δ = 0.32 for glycylhistamine,[22] and here we determined Δ = 0.15. These data show a dramatic decrease of the force of hydrogen-bond with an increasing number of

Table 4. Stability Constants and Derived Data for Co(II), Ni(II), and Cu(II) Complexes of GGHA (as Their Logarithms)[a]

β_{pqr}	Cu(II)	Ni(II)	Co(II)
011	free ligand	7.85(1)	
012		14.66(1)	
111	12.02(3)	10.48(2)	9.96(3)
110	6.61(4)	4.15(4)	3.15(1)
11−1	1.65(9)	−2.87(12)	−5.97(2)
11−2	−2.477(4)	−7.992(4)	−14.98(1)
11−3	−14.34(2)	−19.56(2)	−27.38(8)
pK_{ML}^{MLH}	5.41	6.33	6.81
$pK_{MLH_{-1}}^{ML}$	4.96	7.02	9.12
$pK_{MLH_{-2}}^{MLH_{-1}}$	4.13	5.12	9.01
$pK_{MLH_{-3}}^{MLH_{-2}}$	11.86	11.57	12.4

[a] $\beta_{pqr} = [Cu_pL_qH_r]/[Cu]^p[L]^q[H]^r$, I = 0.1 mol dm^{-3} ($NaClO_4$), T = 298 K, with estimated errors between parentheses (last digit) (calculation of derived data: $pK_{ML}^{MLH} = \beta_{111} - \beta_{110}$; $pK_{MLH_{-1}}^{ML} = \beta_{110} - \beta_{11-1}$; etc.)

Scheme 1. Protonation Pathways in Glycylglycylhistamine

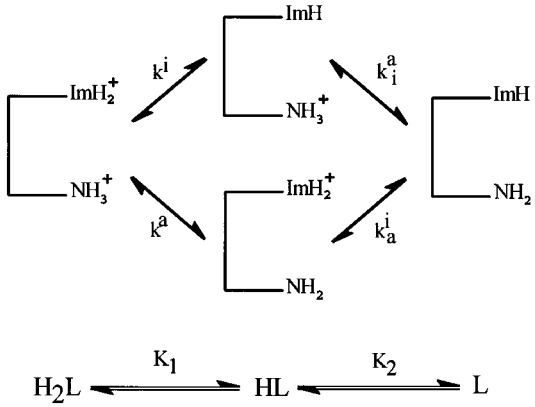

(30) Noszal, B.; Rabenstein, D. L. *J. Phys. Chem.* **1991**, *95*, 4761.

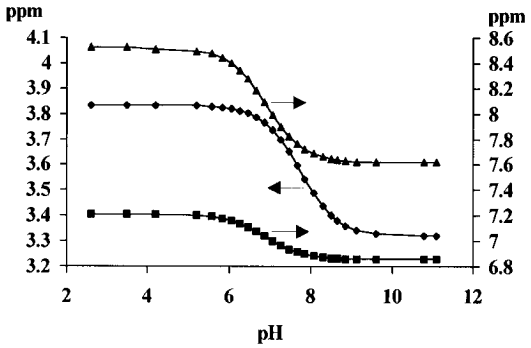

Figure 1. NMR−pH profiles of the imidazole H−C^2 and H−C^5 (upper and lower curves) and the N-terminal methylenic (middle curve) protons.

connecting atoms (3, 6 and 9, respectively) between the two protonation sites.[31]

Metal(II) Coordination. The pH-metric titration curve of an equimolar solution of Cu(II) and GGHA shows a sharp break-point (pH = 6−10) after consumption of 4 equiv of base per metal ion, suggesting the deprotonation and coordination of the two peptide nitrogens besides the terminal amino and imidazole groups (in MLH_{-2} species). At lower metal-to-ligand ratio (R = [M]/[L] = 1:2), the titration curve is consistent with the single excess of ligand besides the complexes formed above when R = 1:1; consequently, the formation of bis-complexes can be neglected. The visible absorption spectra taken at variable pH show the gradual formation of a dominant species in the pH range 5−10, having λ_{max}^{d-d} = 525 nm. In the case of Ni(II), the complex formation starts at higher pH than for Cu(II), but the titration curves become identical above pH 7, suggesting the formation of the same complexes in both systems. The color of Ni(II)-containing solutions changes from light green to yellow between pH 6 and pH 7, indicating the formation of diamagnetic, square-planar complexes (λ_{max}^{d-d} = 425 nm). As expected from the Irving−Williams series, the Co(II) ion forms less stable complexes with GGHA than Cu(II) or Ni(II): the consumption of 4 equiv of base per cobalt(II) ion was detected only at pH 10. In all the systems examined, further deprotonation takes place after pH 10; this can be also followed by the change of visible spectra.

Considering all the facts mentioned above, the pH-metric curves in all systems were best fitted by taking into account six species in the pH range 3 −11.2, differing from each other only in their protonation states: M, MLH, ML, MLH_{-1}, MLH_{-2}, and MLH_{-3}. This set of complexes shows some similarities with other findings in closely related systems, without being however identical to any one of those previously reported. The formation constants determined and the derived pK's for the deprotonation of the successive complexes (e.g. pK_{ML}^{MLH} for the deprotonation of MLH into ML) are listed in Table 4. In all cases, the $pK_{MLH_{-1}}^{ML}$ values are greater than the $pK_{MLH_{-2}}^{MLH_{-1}}$ ones (especially in the case of Ni(II) or Cu(II) ; $\Delta pK = pK_{MLH_{-1}}^{ML} - pK_{MLH_{-2}}^{MLH_{-1}}$ = 1.91 and 0.83, respectively), demonstrating important cooperativity in these two deprotonation steps. The species distribution curves as a function of pH are shown in Figure 2. The MLH_{-2} species is indeed the major complex between pH 5 and pH 11 (in addition to ML and MLH_{-1} in the case of cobalt(II)).

In spite of the great efforts made to study the complex formation of such serum albumin mimicking peptides, little is

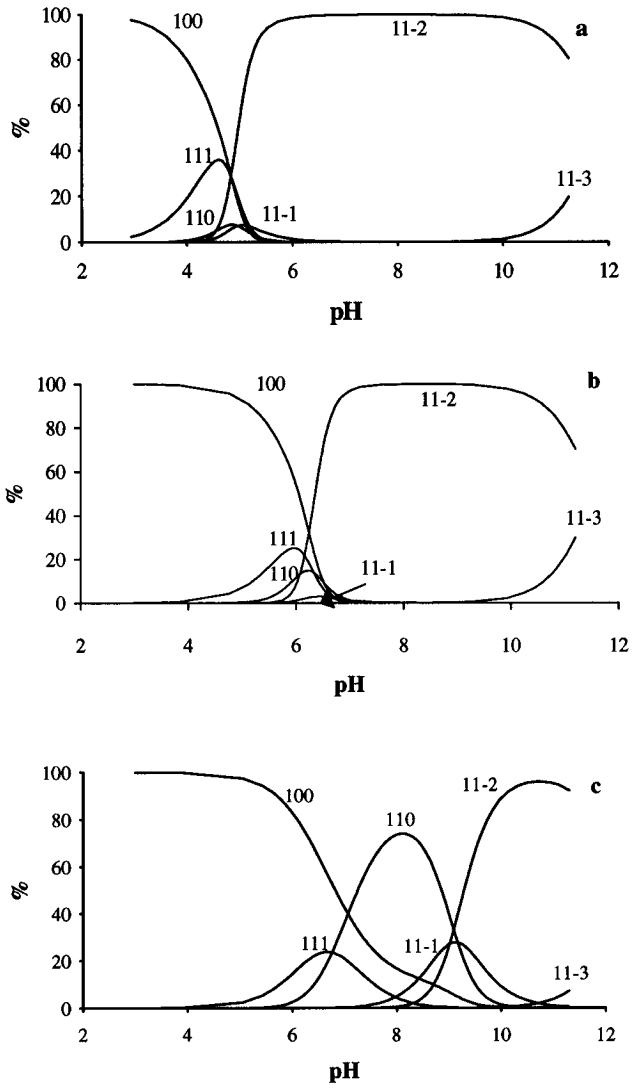

Figure 2. Species distribution curves in Cu(II)−GGHA, Ni(II)−GGHA, and Co(II)−GGHA systems (curves a, b, and c respectively) at 25 °C. [M] = 0.006 mol dm^{-3} and [L] = 0.012 mol dm^{-3}. (Each species $M_pL_qH_r$ is indicated by the set of subscripts p, q, and r).

known about the structure of the species formed, with the exception of MLH_{-2}. Considering the significantly overlapping deprotonations of the imidazole and amino groups in the free ligand, the first metal promoted deprotonation can also occur at either nitrogen, forming two binding isomers (MLH; see Chart 1). In the 2N coordinated ML complexes, all nitrogens in GGHA can be candidates as binding sites. However, in the case of *N*-acetylhistamine, even copper(II) is not able to promote amide deprotonation;[32] thus a {N$^-$,imidazole-N^3} 6-membered chelate formation can be neglected. Among the remaining possibilities, a 5-membered chelate formation {NH_2,N$^-$} (Chart 1, ML(b)) seems to be more probable on thermodynamic ground compared with an amino and imidazole coordinated macrochelate (Chart 1, ML(a)). However, in the case of Co(II)—where the ML complex is the major species at pH ∼ 8—there is a strong argument for such a macrochelate formation: the two further deprotonations of the CoL complex can be assigned higher pK values than those of the free ligand, therefore they can only be attributed to the cobalt(II) promoted deprotonation of the two peptide nitrogens, which are therefore protonated in the CoL species. For the 3N coordinated MLH_{-1} species we

(31) This influence has to act through space (i.e. by hydrogen-bond), since the inductive effect (I$^-$, influence through bond) is negligible after 3−4 nonconjugated connecting atoms.

(32) Sovago, I.; Hartman, B.; Gergely, A. *J. Chem. Soc., Dalton Trans.* **1986**, 235.

Chart 1. Structures Proposed for GGHA Complexes

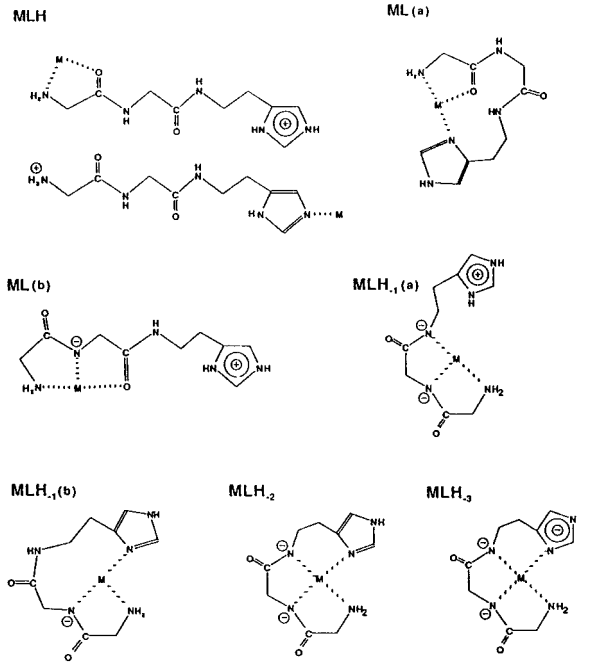

propose also two structures; however, in the case of cobalt(II), the formation of MLH_{-1}(a) structure can be neglected on a similar ground as stated above. One can easily explain the mentioned cooperativity in the deprotonation of ML and MLH_{-1} species, since the simultaneous deprotonation and coordination of the fourth nitrogen in both structures MLH_{-1} a and b (see Chart 1) are extremely favorable. The higher ΔpK value in the case of nickel(II) results from the additional ligand-field stabilization, due to the formation of spin-paired planar nickel-(II) complexes with four nitrogen donor atoms. The species distribution curves show the predominant role of MLH_{-2} in complex formation for all the metal ions. This observation agrees well with most earlier studies concerning serum albumin mimicking peptides. The formation constants determined for $CuLH_{-2}$ and $NiLH_{-2}$, respectively, are slightly lower than those of the corresponding histidine derivatives: $\log\beta_{11-2} = \sim -1.8$ for Cu(II) and $\log\beta_{11-2} = -6.93$ for Ni(II) (see later in the conclusions).

The observed base consumption above pH 10 can be attributed to a further deprotonation of GGHA rather than to the hydrolysis of complexes. Among the SA mimicking peptides, Aiba *et al.* already proposed such a deprotonation[7] for the Cu(II)−Gly-Gly-His, however the reported value $pK^{MLH_{-2}}_{MLH_{-3}} = 10.69$ is too low and seems to be perturbed by the oxidative decarboxylation of Gly-Gly-His.[11]

EPR Spectroscopy. To verify the proposed structures and compositions of complexes formed in solution, spectroscopic measurements have been performed in the case of nickel(II) and copper(II). The first spectroscopically determinable complex is the major species MLH_{-2}. Figure 3 presents the EPR spectra of the equimolar solution of the Cu(II)-GGHA system. The nine sharp and well resolved superhyperfine patterns on the high-field hyperfine line and the EPR parameters determined at pH 8 ($g_o = 2.097(1)$, $A_o = 83.3(4)$ G, and $A_{No} = 13.3(2)$ G) fully support the coordination of four nitrogens in the equatorial plane of copper(II). At higher ligand excess ([Cu]/[L] = 1:50 at pH 8) the spectrum (not shown) practically does not change ($g_o = 2.095(1)$, $A_o = 83.8(4)$ G, and $A_{No} = 13.4(2)$ G). Similarly, no change was observed on visible spectra upon addition of ligand. These facts suggest negligible (if any) bis-complex formation and confirm the presence of only one species, $CuLH_{-2}$, between pH 5−10.

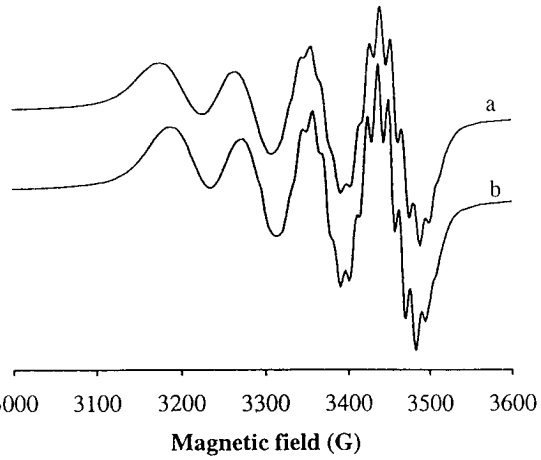

Figure 3. EPR spectra of the Cu(II)−GGHA system ($T = 298$ K, [Cu(II)] = 0.008 mol dm^{-3}, [Cu] = [L] = 1) at pH 8 (a) and 12.5 (b).

With increasing pH above 10 a further base consumption was detected by pH-metry. The visible spectra showed noticeable change in intensity without shift of λ^{d-d}_{max}, while the EPR spectrum of the Cu(II)-GGHA system at pH 12.5 ($g_o = 2.095$-(1), $A_o = 78.7(4)$ G, and $A_{No} = 12.7(2)$ G) (Figure 3b) has a similar pattern as the one at pH 8 (Figure 3a). These facts suggest the same equatorial 4N-coordination in MLH_{-3} species as that already stated for MLH_{-2}.

NMR Spectroscopy. The Cu(II)−GGHA System. ^{1}H-NMR spectroscopy, however, shows some noteworthy features that seem to be accounted for by the existence of traces of labile bis-complexes. The paramagnetic complex $CuLH_{-2}$ cannot be detected because of a lack of sensitivity arising from both low concentration and extreme line-broadening. In this respect, no signal from the ligand is observed in solutions with a metal-to-ligand ratio R equal to unity, between pH 6−10 where $CuLH_{-2}$ is the highly predominant species. Indirect information upon $CuLH_{-2}$ can however be obtained by observing the diamagnetic free ligand L* added in large excess, provided that there is a chemical exchange between free (L*) and bound (in $CuLH_{-2}$) ligand molecules.[33] In the present case, the formation/dissociation process of the complex, which seems necessary for ligand exchange, is presumably immeasurably slow on the NMR time scale, because it requires breaking all four nitrogen to metal bonds simultaneously.[34] However, as suggested first by Pearson and Lanier,[35] multidentate ligands can substitute to each other without the metal ion being fully dissociated at any time. In this case, ligand exchange involves the fast reversible release of one end of a molecule in the complex, followed from time to time by the attachment of a second ligand molecule L* from the bulk solution to the temporarily vacant coordination site. This amounts to a fast preequilibrium in which intermediate bis-complexes are formed by addition of a second ligand molecule L* monodentately bound to the metal. The two ligand molecules (L and L*) around the metal ion may then rapidly compete for the four coordination sites, the whole process ends with the release of either the initial (L) or incoming (L*) molecule. These two events correspond, or not, respectively,

(33) Delpuech, J. J. In *Dynamics of Solutions and Fluid Mixtures by NMR*; Delpuech, J. J., Ed.: John Wiley: New York, 1995; pp 115−119.
(34) Henry, B.; Boubel, J. C.; Delpuech, J. J. *Inorg. Chem.* **1986**, *25*, 623.
(35) Pearson, R. G.; Lanier, R. P. *J. Am. Chem. Soc.* **1964**, *86*, 765.

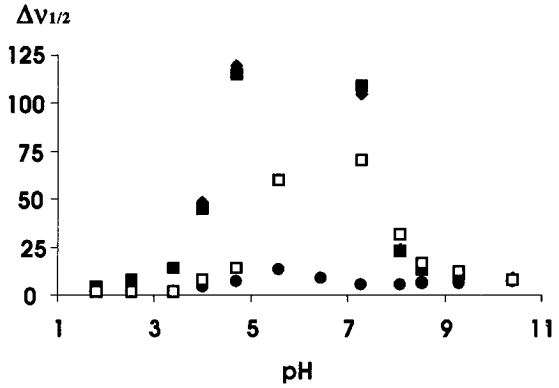

Figure 4. Line-broadenings ($\Delta\nu_{1/2}$) in the Cu(II)−GGHA system as a function of pH at 25 °C ([L] = 50[Cu] = 0.2 mol dm^{-3}) for ^{1}H singlets: C^2−*H* (■) and C^5−*H* (◆) (imidazole ring) ; C^9−H_2 (○) and C^{11}−H_2 (□) (central and terminal glycyl residues, respectively).

to an overall NMR site exchange, written in the present case as

$$CuLH_{-2} + L^* \leftrightarrow CuL^*H_{-2} + L$$

Experimental evidence for such a fast preequilibrium was brought in the case of D_3 tris-complexes of diphosphorylated symmetrical bidentate ligands by DNMR measurements of intramolecular optical inversion between the Λ and Δ enantiomers accompanying the intermolecular ligand exchange.[36]

The ^{1}H-NMR spectra of the Cu(II)-GGHA system with a high excess of free ligand (R = 1:50) shows a severe line-broadening on elevation of the pH from *ca.* 4 to 8, and then a progressive line resharpening at higher pH (Figure 4). Similar observations have been made on the copper(II)−glycylglycylhistidine system.[37] This behavior is reminiscent of the coalescence pattern generally obtained in the special case of one predominant line[33] (that from the free ligand L*) exchanging with the small undetected corresponding line in $CuLH_{-2}$. The predominant line is sharp either in the slow-exchange or the fast-exchange regions, which should correspond to the two observed pH ranges: pH < 8 and pH > 8 *(or vice versa)*. A maximum line-broadening $\Delta\Delta\nu_{1/2}^{max}$ is obtained in between when the NMR exchange rate $1/\tau_M$ (from the paramagnetic to the diamagnetic site) is of the order of $2\pi\Delta\nu_M$. The paramagnetic shift $\Delta\nu_M$ is the frequency shift induced on the observed nucleus of the ligand upon coordination to the copper(II) ion. With $\Delta\Delta\nu_{1/2}^{max}$ on the order of 10^2 Hz in the present case, paramagnetic shifts and exchange rates are approximatively $\Delta\nu_M \approx 5$ kHz and $1/\tau_M \approx 3 \times 10^4$ s^{-1}. These values are of an expected order of magnitude when compared to those obtained for the Cu(II)−L−histidine system,[34] where $1/\tau_M = 7.5 \times 10^5$ s^{-1}. The problem of assigning the slow- and fast-exchange regions on the pH scale was solved by measuring ^{13}C T_1 relaxation times at pH 9.8 in 0.5 molar solutions of GGHA added with increasing amounts of copper(II) (from 0 to 0.022 mol dm^{-3}). The specific relaxation rates $1/T_{1r} \approx 10-40$ s^{-1} thus obtained are easily shown to be approximatively equal to exchange rates in the present conditions; hence, $1/\tau_M \approx 10^1$ - 10^2 s^{-1} at pH 9.8. This shows that the slow-exchange region should be assigned to the higher pH range (pH > 8).

If we come back to the mechanism for ligand exchange proposed above, this means that elevation of the pH should result in decreasing amounts of the labile bis-complexes acting as intermediates in the overall process. This is easily understood if one considers that increasing the acidity of the solution brings about the reversible protonation of any of the four nitrogen sites in $CuLH_{-2}$; this amounts to considering the reversible formation of $CuLH_{-1}$

$$CuLH_{-2} + H^+ \leftrightarrow CuLH_{-1}$$

(see also the speciation curves, Figure 2a). The deprotonation of $CuLH_{-1}$ then follows, for a very small fraction, an unusual pathway, in which an incoming molecule L* binds to the vacant site in $CuLH_{-1}$ (see the formulas MLH_{-1} a and b, Chart 1) so as to yield the intermediate bis-complex $CuLL^*H_{-1}$. A wide range of maximum line broadenings $\Delta\Delta\nu_{1/2}^{max}$ is observed for different protons of GGHA (Figure 4) from about 100−200 s^{-1} for the imidazole ring and the terminal glycyl residue, to 10−20 s^{-1} for the central glycyl residue. These differences presumably show that the two ends of GGHA are involved in a fast exchange of the monodentately bound incoming molecule L* between the bis-complex $CuLL^*H_{-1}$ and the bulk solution.

Figure 5. ^{1}H NMR spectra of GGHA in the presence (b and d) and the absence (a and c) of Ni(II), at pH 10 (a and b) and pH 12.5 (c and d). T = 298 K and [Ni] = [L] = 0.02 mol dm^{-3}. (The signal at 3.7 ppm is the dioxane reference.)

The Ni(II)−GGHA System. The diamagnetic nature of the $NiLH_{-2}$ complex affords an excellent opportunity to study its structure by NMR spectroscopy, even without ligand excess. The gradual increase of the metal-to-ligand ratio R = [Ni^{2+}]:[L] in the GGHA solution (pH = 10) causes important changes in the proton spectrum : the intensity of the free ligand peaks decreases simultaneously with the appearance of new (bonded ligand) signals, until a ratio R = 1:1 is reached, in which case the free ligand signals have disappeared. Since the two sets of lines can be observed separately upon addition of metal ion, the $NiLH_{-2}$ complex is in the slow exchange limit. The ^{1}H-NMR spectra of GGHA in the presence (curves b and d) and absence (a and c) of Ni(II) are shown at pH 10 and 12, respectively, in Figure 5, while the relevant chemical shifts are collected in Table 5. At pH 10, all the proton peaks of the

(36) Rubini, P.; Rodehüser, L.; Delpuech, J. J. *Inorg. Chem.* **1979**, *18*, 2962.
(37) Kuroda, Y.; Aiba, H. *J. Am. Chem. Soc.* **1979**, *101*, 6837.

Table 5. ^{1}H-NMR Chemical Shifts of Free and Ni-Complexed GGHA in D_2O (Ni^{2+} = 0.025 mol dm^{-3}) at Different pH[a]

		C8−H	C9−H	C6−H_2	C5−H_2	C3−H_2	C1−H_2
ligand	pH = 10.0	7.61	6.85_5	2.73	3.40	3.81_5	3.30_5
	pH = 12.5	7.60	6.84	2.72	3.29_5	3.81	3.30
complex	pH = 10.0	7.26	6.81	2.59 or 2.70		3.36	3.12
	pH = 12.5	6.82_5	6.66	2.59 or 2.71		3.35	3.09

[a] The numbering of carbon atoms corresponds to the X-ray study of Cu(H_{-2}GGHA)·$3H_2O$ complex; see Figure 6).

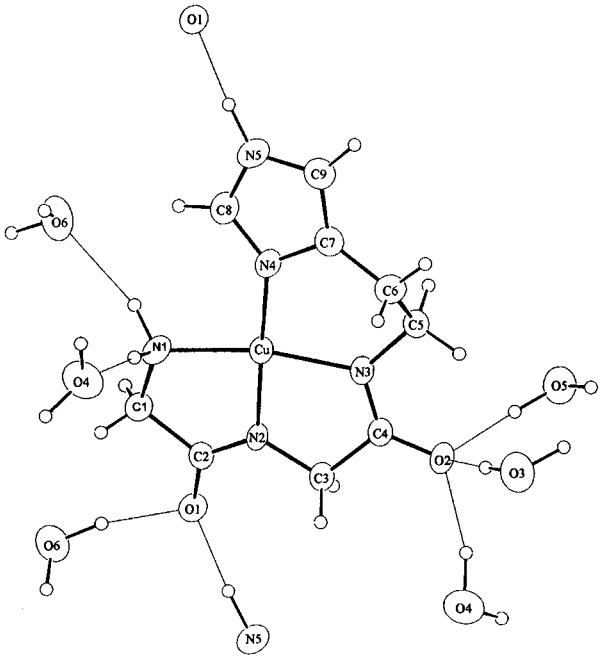

Figure 6. ORTEP drawing of CuGGHAH$_{-2}$·$3H_2O$ with hydrogen bonds.

bonded ligand are significantly shifted upfield, this is the consequence of an expected 4N coordination.

Comparing the ^{1}H-NMR spectra of the Ni(II)−GGHA (R = 1:1) system recorded at pH 10 and 12.5 (Figure 5b,d) allowed us to assign the further consumption of 1 equiv of base above pH 10 to the deprotonation of the imidazole-N^1 nitrogen: the methylenic protons have practically the same chemical shifts, while the imidazole protons are well shifted upfield. The deprotonation of the pyrrolic nitrogen to give the MLH_{-3} species is due to the change of the electronic structure in the imidazole ring upon metal coordination at N^3 nitrogen, with the net effect of lowering the relevant pK to about 12.

Crystal Structure of Cu(GGHAH$_{-2}$)·$3H_2O$ Complex. The structure and atom-labeling of complex is shown in Figure 6. The crystallographic data are collected in Tables 2 and 3. The nature of coordination of GGHA in the $CuLH_{-2}$ complex elucidated above in solution is confirmed by X-ray studies: the copper(II) is tetracoordinated by four nitrogens : amine, two peptide and N4 (or imidazole-N^3 using the IUPAC convention), forming a mildly distorted square planar arrangement. The donor atoms are coplanar to within 0.05 Å. The copper(II)-nitrogen distances are between 1.897 and 2.034 Å. The longest distance is the copper(II)−N1 while the shortest is the copper-(II)−N2 bond. Only the latter (N2) nitrogen is included in two 5-membered chelate rings, this may explain the relatively short bond length. The N−Cu−N (and Cu−N−C) angles also depend on the size of the chelate ring (see Table 4). Most structural parameters presently determined are similar to the analogous Cu(II)−gghma,[14] Ni(II)−Gly-Gly-α-hydroxy-D,L-histamine[38] (Ni(II)−gghh) and Cu(II)−α,β-didehydro-Gly-Gly-histamine[16] (Cu(II)−dggh) complexes—the latter two compounds formed from the appropriate Gly-Gly-His complexes undergoing an oxidative decarboxylation—however there are some notable differences: (i) in Cu−gghma there is an axial water coordination, and therefore the copper(II) ion is out of the plane determined by the four coordinated nitrogens, while in Cu-GGHA the copper(II) is strictly four coordinated and is exactly in the least-squares plane of the four coordinated nitrogens; (ii) the M(II)−N distances are close to each other in the three copper(II) complexes, but much shorter bonds were determined in Ni(II)−gghh as a consequence of spin-paired planar structure; (iii) there are many hydrogen bonds in the crystal structure of Cu(II)−GGHA, and all proton acceptor and donor atoms are involved at least in one hydrogen bond. A very strong intermolecular hydrogen bond was detected between the proton (HN5 in Table 4) of the imidazole pyrrolic nitrogen and the carbonyl oxygen O1 of another molecule: the H···O distance is 1.72 Å, while the analogous distance in Cu-gghma is 2.12 Å.

Conclusion

In order to get further information about the structure of and the role of the carboxylate group in the metal complexes of SA mimicking peptides, we studied the proton and metal ion interactions of GGHA. The two protonation steps—over the amino (NH_2) and imidazole (Im H) groups—in the free ligand overlap significantly, producing an alternative unexpected microprotonation pathway. This results into the presence of a microspecies, monoprotonated on the imidazole ring (Im H_2^+ − NH_2) at the extent of *ca*. 16%, suggesting the possibility for additional amino coordination even at low pH (Chart 1).

Due to the multidentate nature of GGHA (and of all SA mimicking peptides), monomeric complexes, more or less deprotonated, formed in all systems. At physiological pH, the MLH_{-2} species is predominant in the case of Ni(II) and Cu-(II), while, in Co(II)−containing systems, CoL is the predominant complex with a macrochelate coordination of terminal amino and imidazole nitrogens. Above pH 10, in all the systems studied in this paper, we observed a new deprotonation which was assigned to the N^1 nitrogen of the imidazole ring, without metal coordination. The stability constants determined by us, showed a somewhat lower coordination ability of GGHA in all species, compared to the analogous ligands having additional O-donor group(s) (amide and/or carboxylate), e.g. Gly-Gly-His,[7−12] gghma[13] and aahma,[15] where the observed stability constants are : log β_{11-2}: ≈ −1.8, −0.48, and −0.55 (against −2.48 for GGHA). This deviation could be attributed to a weak axial coordination of the O-donor group. However, under these conditions, the above sequence of stability constants should imply that the carboxylate end of Gly-Gly-His binds less strongly than the amide carbonyl oxygen of gghma (or aahma), this is unlikely on electrostatic grounds. Another piece of evidence against an additional coordination of O-donor group comes from the observation of the same stability sequence (log β_{11-2} = −7.99, −6.93, and −5.94 for GGHA, Gly-Gly-His[18] and aahma,[15] respectively) in the case of nickel(II) complexes,

(38) Bal, W.; Djuran, M. J.; Margerum, D. W.; Gray, E. T.; Mazid, M. A.; Tom, R. T.; Nieboer, E.; Sadler, P. J. *J. Chem. Soc., Chem. Commun.* **1994**, 1889.

where, however, the $NiLH_{-2}$ species are generally reported to have a 4N coordinated square planar structure and where additionnal axial coordination is not probable. Considering the above facts, the effect of the free carboxylate or of the amide side chain seems to arise from an increased acidity of the nearby peptide nitrogen, rather than from a direct coordination.

Definite evidence for tetracoordination by four nitrogen atoms (amino, two peptide and imidazole-N^3) in MLH_{-2} species is brought both by the superhyperfine EPR pattern and the X-ray structure of the copper (II) complex. Bis-complexes in our systems were present only at very low concentration, even with high ligand excess. Their presence, in undetectable amounts, was required to account for unusual DNMR patterns in the copper(II)−GGHA system between pH 4 and pH 10 with a metal-to-ligand ratio of 1:50. The complex $NiLH_{-2}$ could be observed directly by ^1H NMR due to its diamagnetic nature and to slow ligand exchange. NMR measurements upon further additions of base to a $NiLH_{-2}$ solution produced direct evidence for the deprotonation of the pyrrolic nitrogen to give the MLH_{-3} species.

Acknowledgment. Financial support from the Centre National de la Recherche Scientifique and the Hungarian Research Fundation (OTKA F 014954) is gratefully acknowledged.

Supporting Information Available: Lists positional and anisotropic thermal parameters, hydrogen atom parameters, bond distances, bond angles, torsion angles and least-squares planes of the $CuGGHAH_{-2}$ complex (36 pages). Ordering information is given on any current masthead page.

IC950373E